JACC: BASIC TO TRANSLATIONAL SCIENCE VOL. 9, NO. 12, 2024
© 2024 THE AUTHORS. PUBLISHED BY ELSEVIER ON BEHALF OF THE AMERICAN COLLEGE OF CARDIOLOGY FOUNDATION. THIS IS AN OPEN ACCESS ARTICLE UNDER THE CC BY-NC-ND LICENSE (http://creativecommons.org/licenses/by-nc-nd/4.0/).

ORIGINAL RESEARCH - PRECLINICAL

# Exercise Therapy Rescues Skeletal Muscle Dysfunction and Exercise Intolerance in Cardiometabolic HFpEF

Heather Quiriarte, MS,[a,b] Robert C. Noland, PhD,[c] James E. Stampley, PhD,[b] Gregory Davis, MS,[b] Zhen Li, PhD,[d] Eunhan Cho, PhD,[b] Youyoung Kim, MS,[b] Jake Doiron, BS,[a,e] Guillaume Spielmann, PhD,[b] Sujoy Ghosh, PhD,[f] Sanjiv J. Shah, MD,[g] Brian A. Irving, PhD,[b] David J. Lefer, PhD,[d] Timothy D. Allerton, PhD[a,h]

## VISUAL ABSTRACT

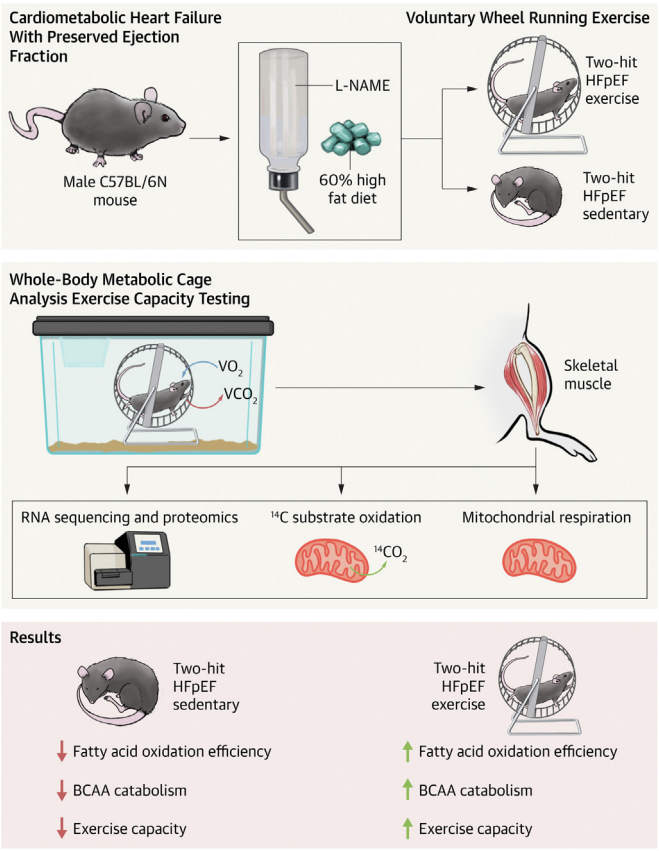


Quiriarte H, et al. JACC Basic Transl Sci. 2024;9(12):1409–1425.

## HIGHLIGHTS

- **Skeletal muscle metabolism is an important factor for exercise capacity in cardiometabolic HFpEF but is not well understood.**
- **Using state-of-the-art metabolic cage technology and a multiomic approach, we define a metabolic signature of skeletal muscle dysfunction and exercise intolerance in a mouse "2-hit" model of cardiometabolic HFpEF.**
- **We then show voluntary wheel running exercise restores skeletal muscle fatty acid and BCAA substrate use and improves exercise capacity without significant improvement in cardiac hemodynamic function.**
- **FAO and BCAA catabolic pathways are potentially important targets to improve exercise intolerance in cardiometabolic HFpEF.**

ISSN 2452-302X https://doi.org/10.1016/j.jacbts.2024.07.009

JACC: BASIC TO TRANSLATIONAL SCIENCE VOL. 9, NO. 12, 2024
DECEMBER 2024:1409–1425

**ABBREVIATIONS AND ACRONYMS**

**ADP** = adenosine diphosphate

**BCAA** = branched-chain amino acid

**ETC** = electron transport chain

**Ex** = exercise (group)

**FAO** = fatty acid oxidation

**HFD** = high-fat diet

**HFpEF** = heart failure with preserved ejection fraction

**$J_{O2}$** = oxygen flux

**L-NAME** = N(ω)-nitro-L-arginine methyl ester

**LVEDP** = left ventricular end-diastolic pressure

**NADH** = nicotinamide adenine dinucleotide plus hydrogen

**PBS** = phosphate-buffered saline

**Sed** = sedentary (group)

**SUMMARY**

Exercise intolerance, a hallmark of heart failure with preserved ejection fraction (HFpEF) exacerbated by obesity, involves unclear mechanisms related to skeletal muscle metabolism. In a "2-hit" model of HFpEF, we investigated the ability of exercise therapy (voluntary wheel running) to reverse skeletal muscle dysfunction and exercise intolerance. Using state-of-the-art metabolic cages and a multiomic approach, we demonstrate exercise can rescue dysfunctional skeletal muscle lipid and branched-chain amino acid oxidation and restore exercise capacity in mice with cardiometabolic HFpEF. These results underscore the importance of skeletal muscle metabolism to improve exercise intolerance in HFpEF. (JACC Basic Transl Sci 2024;9:1409–1425)
© 2024 The Authors. Published by Elsevier on behalf of the American College of Cardiology Foundation. This is an open access article under the CC BY-NC-ND license (http://creativecommons.org/licenses/by-nc-nd/4.0/).

Heart failure with preserved ejection fraction (HFpEF) has become a major health care problem linked to the growing incidence of obesity, hypertension, and sedentary lifestyles.[1] HFpEF accounts for ∼50% of all heart failure cases and affects ∼3 million people in the United States.[2] Patients with HFpEF experience a high rate of mortality and poor quality of life.[3-5] Despite the high phenotypic diversity of HFpEF, exercise intolerance is a cardinal symptom of all HFpEF phenogroups. In the cardiometabolic HFpEF phenogroup (ie, obesity-associated), exercise intolerance is more severe than in other HFpEF groups and limits the ability to engage in exercise and activities of daily living.[6-9]

Numerous reports suggest that noncardiac factors promote exercise intolerance in cardiometabolic HFpEF.[6,7,10-13] Several groups have demonstrated skeletal muscle mitochondrial dysfunction, poor muscle quality, and reduced capillary density in patients with HFpEF when compared to healthy control patients.[13-15] Rapid depletion of high-energy phosphate in skeletal muscle is also noted as a source of fatigue and exercise intolerance in HFpEF.[16] These studies, along with reports of increased serum acylcarnitine levels in patients with HFpEF, strongly suggest a limitation in skeletal muscle fatty acid oxidation (FAO).[17-19] Additionally, branched-chain amino acids (BCAAs) have also been shown to be elevated in the plasma of patients with HFpEF, potentially owing to reduced oxidation in the skeletal muscle.[18,20] This may have serious implications for exercising skeletal muscle and muscle protein synthesis. These markers of inefficient β-oxidation and obesity-related metabolic dysfunction are closely correlated with reduced exercise capacity in HFpEF.[15,16,18,21] These studies indicate that impaired skeletal muscle bioenergetics contribute to exercise intolerance in HFpEF.

Exercise capacity is a sensitive prognostic indicator of quality of life, morbidity, and mortality in HFpEF.[22,23] Exercise training is recommended as a front-line strategy for chronic HFpEF primarily because of its positive impact on cardiorespiratory fitness and quality of life.[24] Greater cardiorespiratory fitness is associated with increased long-term survival in HFpEF; however, exercise intolerance remains a major barrier for patients with HFpEF to engage in regular exercise training.[25] Recent progress in the pharmacologic treatment of HFpEF highlights the potential of targeting metabolic dysfunction as a promising therapeutic direction.[26-29] Unlike pharmacotherapy, exercise training promotes cardiorespiratory fitness and mitochondrial function and improves skeletal muscle substrate metabolism. In patients

From the [a]Vascular Metabolism Laboratory, Pennington Biomedical Research Center, Baton Rouge, Louisiana, USA; [b]Department of Kinesiology, Louisiana State University, Baton Rouge, Louisiana, USA; [c]Skeletal Muscle Metabolism Laboratory, Pennington Biomedical Research Center, Baton Rouge, Louisiana, USA; [d]Department of Cardiac Surgery, Smidt Heart Institute, Cedars-Sinai Medical Center, Los Angeles, California, USA; [e]Department of Pharmacology and Experimental Therapeutics, Louisiana State University Health Sciences Center, New Orleans, Louisiana, USA; [f]Bioinformatics and Computational Biology Core, Pennington Biomedical Research Center, Baton Rouge, Louisiana, USA; [g]Division of Cardiology, Department of Medicine, Northwestern University, Feinberg School of Medicine, Chicago, Illinois, USA; and the [h]Louisiana State University Cardiovascular Center of Excellence, New Orleans, Louisiana, USA.

The authors attest they are in compliance with human studies committees and animal welfare regulations of the authors' institutions and Food and Drug Administration guidelines, including patient consent where appropriate. For more information, visit the Author Center.

Manuscript received April 15, 2024; revised manuscript received July 23, 2024, accepted July 23, 2024.

with HFpEF, exercise training improves skeletal muscle function, exercise capacity, and quality of life.[30-32] Despite these reports, very little is known about the molecular and metabolic signature of skeletal muscle dysfunction, and the adaptations to exercise training, in HFpEF.

In the current investigation, we sought to determine substrate oxidation, transcriptional signatures, and proteomic pathways altered in the skeletal muscle of the "2-hit" mouse model of cardiometabolic HFpEF. With these observations in hand, we tested the hypothesis that exercise training would rescue skeletal muscle metabolic dysfunction in HFpEF and restore exercise capacity in this novel mouse model of HFpEF.

## METHODS

**ANIMAL MODEL AND STUDY DESIGN.** Eight-week-old C57BL/6N male mice were purchased from Charles River Laboratories, and after a 1-week acclimation period, mice were randomly assigned to a control group where they were maintained on a chow diet (Purina, 5001) with regular drinking water or a 60% high-fat diet (HFD) (Research Diet, D12492) and N(ω)-nitro-L-arginine methyl ester (L-NAME) in (0.5 g/L, pH to 7.4) supplemented drinking water to induce HFpEF.[33-37] The L-NAME water was contained in a dark bottle and changed every 3 days. Mice were multihoused for the first 4 weeks and then moved to single-housed training cages (n = 10 per group) for 1 week before starting the metabolic cage experiment. After completing the 1-week metabolic cage experiment, mice from both groups (control and HFpEF) continued their respective treatment for an additional 5 weeks.

**WHEEL RUNNING EXERCISE TRAINING.** A group of HFpEF (HFD+L-NAME) mice were randomly assigned to a wheel running cage to engage in voluntary wheel running exercise (Ex) (n = 13) or to a standard cage with no running wheel (Sed) (n = 13) for the remaining 5 weeks of the experiment. Mice in the Sed group were single-housed to mimic the stress of single-housing conditions. A follow-up metabolic cage (n = 8 per group) experiment was performed during the final week (week 10) of the experiment to determine the impact of exercise training on wheel running performance and metabolic parameters. A malfunction occurred in 1 metabolic cage in the Sed group; therefore, data for 7 mice are reported. Body weight, food, and water intake were measured and recorded weekly. Body composition data were collected weekly via nuclear magnetic resonance (Bruker). Grip force production was measured by force meter (Bioseb, Harvard Apparatus) taking the average of 3 attempts. At the end of the experiment, mice were euthanized by isoflurane administration with cardiac puncture.

**VOLUNTARY EXERCISE CAPACITY TEST: METABOLIC CAGE EXPERIMENTS.** Mice were housed in metabolic cages (Promethion Metabolic Analyzer, Sable Systems International) at room temperature (20-22 °C) for 1 week. Continuous measurements of oxygen consumption ($V_{O_2}$) and carbon dioxide production ($V_{CO_2}$) were performed and averaged every 5 minutes. The volumes of $V_{O_2}$ and $V_{CO_2}$ were used to calculate energy expenditure and respiratory exchange ratio.[38] Spontaneous physical activity, behavioral activity (eating, drinking, resting), and voluntary wheel running were continuously monitored by beam breaks (x-, y-, and z-axes) and by electronic read switch for wheel running counts. Behavioral analysis was performed using Sables Systems Ethoscan. Wheel running energy expenditure and substrate oxidation were calculated as we and others have previously reported.[39,40] The follow-up metabolic cage experiment was conducted in both Sed and Ex mice between weeks 9 and 10 of the experiment. Both groups were placed in cages with locked running wheels for the first 3 days of the experiment to determine resting metabolic measurements and spontaneous physical activity. Running wheels were then unlocked for the next 4 days to determine wheel running performance. The Pennington Biomedical Research Center Institutional Animal Care and Use Committee approved all experiments.

**SUBSTRATE OXIDATION.** Substrate oxidation was measured in skeletal muscle homogenates (mixed gastrocnemius) using $^{14}C$ labeling of pyruvate, leucine, and palmitate.[41-46] Briefly, gastrocnemius homogenates were incubated in the presence of an oxidation buffer containing [1-$^{14}C$] palmitate (0.2 mmol/L), [3-$^{14}C$]pyruvate (1 mM), and [U-$^{14}C$] leucine (0.1 mM) at 0.5 μCi/mL$^{-1}$ (American Radiolabeled Chemicals) for 30 minutes (palmitate and pyruvate) or 2 hours (leucine) at 37 °C. The reaction was terminated by the addition of 100 μL of 70% perchloric acid. Liberation of $^{14}CO_2$ was trapped in 200 μL of 1N NaOH and was used to measure complete oxidation. Acidified samples used to assess palmitate oxidation were centrifuged (10 minutes, 4 °C, 20,000*g*) and 50 μL of the supernatant was used to measure acid-soluble metabolites as an index of incomplete palmitate oxidation. Samples containing $^{14}CO_2$ and $^{14}C$-acid-soluble metabolites were placed in

scintillation vials containing 4 mL Uniscint BD (National Diagnostics) and radioactivity was measured on a scintillation counter.

**HIGH-RESOLUTION RESPIROMETRY.** Immediately postsacrifice, soleus and gastrocnemius were excised and placed in ice-cold relaxation and biopsy preservation buffer (BIOPS, 10 mmol/L Ca-ethylene glycol tetra-acetic acid buffer, 0.1 μmol/L free calcium, 20 mmol/L imidazole, 20 mmol/L taurine, 50 mmol/L K-2-[N-morpholino]ethane sulfonic acid, 0.5 mmol/L dithiothreitol, 6.56 mmol/L $MgCl_2$, 5.77 mmol/L adenosine triphosphate, 15 mmol/L phosphocreatine, pH 7.1). Subsequently, soleus and gastrocnemius were dissected in BIOPS on ice under stereomicroscopy to acquire small fiber bundles (~1-3 mg per bundle). The fiber bundles were placed in fresh ice-cold BIOPS buffer with 50 μg/mL of saponin and placed on an orbital shaker for 30 minutes to chemically permeabilize the plasma membrane.[47] The fiber bundles were then washed in ice-cold MiR05 (MiR05 Kit, Oroboros Instruments; 0.5 mmol/L ethylene glycol tetra-acetic acid, 3 mmol/L $MgCl_2$, 60 mmol/L lactobionic acid, 20 mmol/L taurine, 10 mmol/L $KH_2PO_4$, 20 mmol/L N-2-hydroxyethylpiperazine-N′-2-ethanesulfonic acid, 110 mmol/L sucrose, 1 g/L fatty acid-free bovine serum albumin, pH 7.1) for ~15 minutes. The fiber bundles were then blotted dry for 40 seconds on Whatman paper and weighed on an analytical balance (Mettler Toledo) to the nearest 0.01 mg. The fiber bundles were placed into 2 independent oxygraph chambers with MiR05 supplemented with 3 mg/mL creatine monohydrate and 25 μmol/L blebbistatin (a myosin adenosine triphosphatase inhibitor) for duplicate measurements. The respiratory measurements were made with $O_2$ concentrations between ~425 and 150 μmol/L $O_2$. We measured oxygen flux ($J_{O2}$) during LEAK (state 4) and OXPHOS capacity (state 3) coupling control states. The following titration protocol was adapted from Hahn et al.[48] After initial stabilization, we titrated in pyruvate (10 mmol/L), malate (1 mmol/L), and glutamate (10 mmol/L) in the absence of adenosine diphosphate (ADP) to measure nicotinamide adenine dinucleotide plus hydrogen (NADH)-Linked LEAK $J_{O2}$. Next, we titrated a submaximal bolus of ADP (250 μmol/L) ADP-$Mg^{++}$, followed by a saturating bolus of ADP-$Mg^{++}$ (5 mmol/L) to measure submaximal and maximal NADH-Linked OXPHOS $J_{O2}$.[49] We then titrated in 10 μmol/L cytochrome C to assess the mitochondrial membrane integrity. Next, we titrated in succinate (10 mmol/L) to measure NADH+S-Linked OXPHOS $J_{O2}$. We then titrated in 0.5 μmol/L rotenone to inhibit complex I to measure S-Linked OXPHOS $J_{O2}$. Finally, we added 2.5 μmol/L antimycin A to measure residual $O_2$ consumption. The $J_{O2}$ in the permeabilized muscle fibers was acquired and calculated using DatLab 7.4 software (Oroboros Instruments) and was corrected for residual $O_2$ consumption. We subsequently normalized the $J_{O2}$ per milligram wet-weight ($pmol \cdot s^{-1} \cdot mg^{-1}$). We also corrected all measurements for daily room air calibrations as well as routine instrumental background and zero calibrations. All respirometry measurements and analyses were conducted in a blinded fashion.

**RNA ISOLATION AND RNA-SEQUENCING.** RNA was isolated from skeletal muscle (gastrocnemius) according to established methods.[50,51] Library construction was performed using Lexogen Quant-Seq with 50-base pair forward reads. Sequencing and initial data processing were performed on an Illumina NextSeq instrument according to previously established methods.[52,53] Data were analyzed using STAR software (Illumnia) for alignment, collapse_umi_bam to eliminate polymerase chain reaction duplicate reads, HtSeq for counting reads per gene, DESeq2 to determine differential expression (absolute fold-change >1.5, Benjamini-Hochberg corrected false discovery rate cutoff at 0.1). Raw gene counts were $log_2$ transformed with $P_{adjusted}$ values <0.01. Pathway enrichment analysis was performed using globaltest software in R (version 4.3.2, R Foundation). Ingenuity Pathway Analysis Software (Qiagen) was used to determine canonical pathways as previously established.[54]

**IMMUNOBLOTTING.** Skeletal muscle (gastrocnemius) was snap frozen and liquid nitrogen. Skeletal muscle samples were pulverized in liquid nitrogen and homogenized in immunoprecipitation buffer. Protein concentrations were quantified using a Peirce 660-nm protein assay kit (Thermo Fisher Scientific). A total of 50-100 μg of protein were loaded on 8%-16% Treis-Glycine Plus Midi Gels (Invitrogen) and transferred onto 0.45-μm nitrocellulose membranes (Bio-Rad Laboratories). Membranes were blocked with Everyblot blocking buffer (Bio-Rad) and probes with primary antibodies for 1 hour. Proteins were detected using peroxidase-conjugated affiniPure Goat Anti-Rabbit IgG secondary antibody (Jackson ImmunoResearch). Blot imaging and quantification were acquired using a Thermo iBright imager and iBright Analysis software (Thermo Fisher Scientific). Total protein for normalization was performed using a nonstain protein labeling reagent (Invitrogen) according to the manufacturer's instructions.

**PROTEOMICS.** A total of 50 μg of homogenized gastrocnemius was used for proteomics analysis.

Each sample was mixed with 150 μL 1% sodium dodecyl sulfate, 20 μL 10% sodium dodecyl sulfate, and 20 μL of bovine serum albumin internal standard (1 μg). The samples were mixed, heated at 70 °C, and precipitated with acetone overnight. The precipitate was reconstituted in 50 μL of Laemmli sample buffer and 20 μL (one-half the sample) run 1.5 cm into a sodium dodecyl sulfate-polyacrylamide gel electrophoresis gel. Each 1.5-cm lane was cut as a sample, cut into smaller pieces, washed, reduced, alkylated, and digested with 1 μg trypsin overnight at room temperature. Peptides were extracted from the gel in 50% acetonitrile, the extracts taken to dryness by Speedvac, and reconstituted in 200 μL 1% acetic acid for analysis.

The TSQ Quantiva instrument (Thermo Fisher Scientific) was used in the Selection Reaction Monitoring mode with Q1 and Q3 resolution = 0.7 full width at half maximum. Each Selection Reaction Monitoring method was constructed with the program Skyline (SCIEX) in a series of steps that select and validate the best-responding peptides for each protein target. Two to 3 peptides were used for each protein measurement. Data were analyzed using the program Skyline. This program finds and integrates the chromatographic peak areas for peptides previously developed as quantitative markers for each protein. QEx plus instrument was used in the Data Independent Analysis mode with a 20 m/z window working from 350 to 950 m/z. The orbitrap was operated at a resolution of 17,500. A full scan spectrum at a resolution of 70,000 was acquired each cycle. These conditions give 7-8 data points across our typical 30-second chromatographic peaks. Data were analyzed using the program DIANN. This program uses neural network methods to analyze the Data Independent Analysis datasets vs the respective Uniprot proteome database from Embl.

**ORAL GLUCOSE AND INSULIN TOLERANCE TESTS.** Oral glucose tolerance testing was performed 8 weeks after the HFD and L-NAME (3 weeks after starting exercise). Mice were fasted for 4 hours and gavaged with glucose 3.5 g/kg lean mass. Tail vein blood was collected before and 15, 30, 60, 90, and 120 minutes post glucose gavage. Insulin tolerance was tested 9 weeks after HFD and L-NAME treatment (4 weeks after starting exercise). Insulin was injected at a dose of 1.5 U/kg lean mass. Tail vein blood was collected before and 10, 20, 40, 60, and 120 minutes post insulin injection.

**INVASIVE HEMODYNAMICS.** Mice were fully anesthetized using isoflurane (3.0%) until unresponsive. When mice were unresponsive to stimuli, the left common carotid artery was surgically exposed, and a 1.2-F pressure catheter (Transonic) was introduced into the carotid artery and advanced into the aorta. Aortic systolic and diastolic blood pressures were then measured and recorded. The catheter was then advanced into the left ventricular cavity and left ventricular end-diastolic pressure (LVEDP) and tau were measured followed by thoracotomy.

**IMMUNOHISTOCHEMISTRY.** Skeletal muscle (tibialis anterior) was cryosectioned and stored at −80 °C until staining. Muscle sections were stained for fiber type according to previously established methods with some modifications.[55,56] Muscle sections were rehydrated in Dulbecco phosphate-buffered saline (PBS) (Gibco) then blocked with 10% goat serum for 30 minutes. After, slides were washed with PBS, then incubated in a primary antibody cocktail with 10% goat serum at room temperature overnight. Primary antibodies were acquired from the Developmental Studies Hybridoma Bank. Mouse $IgG_{2B}$ monoclonal antibody anti-MyHC-I (1:40; BA-D5), mouse $IgG_1$ monoclonal anti-MyHC-IIA (1:200; SC-71), mouse IgM monoclonal anti-MyHC-IIB (1:100; BF-F3) were used for staining type I, IIA, and IIB fibers, respectively. A rabbit polyclonal antibody (1:154; Abcam, #ab11575) was used to stain for laminin. After washing in PBS, sections were incubated in secondary antibody solution containing AF568 (Thermo Fisher Scientific, A-21124) $IgG_1$ (1:100), AF488 (Thermo Fisher Scientific, A-21042) GaM IgM (1:00), Dylight 405 (Jackson ImmunoResearch, 115-475-207) IgG (1:100), AF647 (Jackson ImmunoResearch, 711-605-152) DaR IgG (1:200) for 1 hour. After PBS washes (3 × 5 minutes) sections were dehydrated 2 × 2 minutes in 70% ethyl alcohol and 2 × 2 minutes in 100% ethyl alcohol. Coverslips were then attached to air-dried slides with Prolong Diamond Antifade Mountant (Invitrogen, P36965). Section images were acquired with a Zeiss Axioscan Slide Scanner and analyzed ImageJ (National Institutes of Health) to quantify muscle fiber type proportion and fiber cross-sectional area.

**STATISTICAL ANALYSIS.** The normality of data distribution was determined using D'Agostino and Pearson and Shapiro-Wilk tests. Analysis of energy expenditure was performed using analysis of covariance according to established guidelines.[57,58] Total body mass, lean mass, fat mass, and total activity were used as covariates in the analysis of covariance model. Mixed-effects model for repeated measures was used to analyze longitudinal data such as oral glucose. Fixed effects included continuous variables of time point, group, and group-by-time interaction. One-way analysis of variance with a Tukey multiple

comparison test was used to determine group differences among chow, HFD, L-NAME, and HFpEF groups when applicable. The trapezoidal method was used to determine the area under the curve. Simple linear regression was performed to evaluate slopes and correlation derived from continuous data. Heat maps and enrichment plots were made using SRplot (Bioinformatics). All data are presented as mean ± SD. Statistical significance was determined as $P < 0.05$. Statistical analysis was performed using Prism 10 software (GraphPad Software). Energy expenditure analysis of covariance was performed using the National Institute of Diabetes and Digestive and Kidney Diseases Mouse Metabolic Phenotyping Centers using their Energy Expenditure Analysis page and supported by grants DK076169 and DK115255.

## RESULTS

**DYSREGULATED FATTY ACID AND BCAA CATABOLISM ARE METABOLIC SIGNATURES OF HFpEF SKELETAL MUSCLE.** Dysregulated skeletal muscle metabolism and mitochondrial function are significantly correlated to peak oxygen consumption and 6-minute walk distance in patients with HFpEF.[13,15] Other studies have shown cardiac metabolic signatures in HFpEF related to dysregulation in fatty acid metabolism.[17-20] However, there is a paucity of data on skeletal muscle metabolism in preclinical models of cardiometabolic HFpEF, limiting the translational value of these models. We conducted a multiomic approach to determine the molecular and metabolic regulation of skeletal muscle after 10 weeks of HFD and L-NAME treatment. As we, and others, have previously demonstrated,[35,37,59] the combination of HFD and L-NAME induces cardiometabolic HFpEF characterized by obesity, insulin resistance, exercise intolerance, and diastolic dysfunction (Supplemental Figures 1 to 3). We performed bulk RNA-sequencing and proteomics (untargeted and targeted) on the skeletal muscle (gastrocnemius) of HFpEF and control mice (**Figure 1A**). The transcriptional signature of the 2-hit HFpEF model is characterized by a high enrichment of metabolic and bioenergetic signaling pathways (**Figures 1B to 1D**). Genes linked to mitochondrial β-oxidation (ie, *Acaa2, Acsl, Acot2, Hadh, Hadha, Hadhb*) and the regulation of lipid metabolism by *PPARα* (*Acadm, Acsl1, Cpt2, Pex11a, Slc27a1*) were significantly up-regulated ($z$-score = 2.0-3.0) in HFpEF. Likewise, genes that regulate fatty acid transport (ie, *Acsl5, Cd36, Cpt1, Cpt2, Fabp3*) were also significantly increased in the HFpEF group. BCAA metabolism pathways (ie, *Acaa2, Acadsb, Bcat2, Ivd*) were mostly down-regulated in HFpEF vs control skeletal muscle. Pathways related to blood clotting, peroxisome proliferator-activated receptor signaling, oxidative phosphorylation, and fatty acid oxidation were highly enriched when comparing control (chow) mice to mice treated with HFpEF (up-regulated), HFD alone (up-regulated), and L-NAME alone (down-regulated) (Supplemental Figure 4). Untargeted proteomics revealed 269 differentially regulated proteins between HFpEF and control skeletal muscle. In agreement with gene expression, the proteins related to metabolic pathways (β-oxidation, tricarboxylic acid cycle, and BCAA catabolism) were highly represented (**Figure 1E**). When comparing similar genes that were differentially regulated at the messenger RNA and protein level, 36 targets emerged (**Figure 1F**). These genes and proteins demonstrated an up-regulation of β-oxidation and down-regulation of BCAA catabolism (**Figure 1G**).

Next, we determined whether the changes in molecular signaling result in alterations in skeletal muscle palmitate and leucine oxidation. No differences were detected in the complete FAO (**Figure 1H**), but incomplete FAO to $^{14}$acid-soluble metabolites was increased and leucine oxidation was decreased in HFpEF skeletal muscle (**Figures 1I and 1J**). When compared to diet-induced obese mice (HFD-treated) dysregulation of skeletal muscle substrate use persisted (Supplemental Figure 5). High-resolution respirometry of permeabilized soleus fibers revealed HFpEF mice have increased mitochondrial uncoupled respiration (LEAK state) and reduced respiratory control ratio (OXPHOS/LEAK) when compared to control mice (**Figures 1K and 1L**).

**WHEEL RUNNING EXERCISE IMPROVES PHYSICAL CAPACITY IN HFpEF.** We conducted five weeks of exercise training (voluntary wheel running, Ex) after the onset of HFpEF (**Figure 2A**). At the end of the exercise training period, Ex mice had a lower body mass (**Figure 2B**) and body fat (**Figure 2C**) and increased lean mass (**Figure 2D**), soleus, and gastrocnemius wet weight (**Figures 2E and 2F**) when compared to the Sed group. Forelimb grip force production measured was also significantly increased in the Ex group (**Figure 2G**). Oral glucose tolerance (group effect: $P < 0.05$) (**Figures 2I and 2H**) and insulin tolerance (**Figures 2I and 2J**) were improved in exercised HFpEF mice.

To determine the impact of wheel running exercise on physical capacity and in vivo exercise performance, both groups were housed in metabolic cages with locked running wheels for the first 3 days to monitor all resting and nonexercise activity and washout the previous bout of exercise in the Ex

**FIGURE 1** Mitochondrial Dysfunction and Impaired Substrate Use in HFpEF Skeletal Muscle

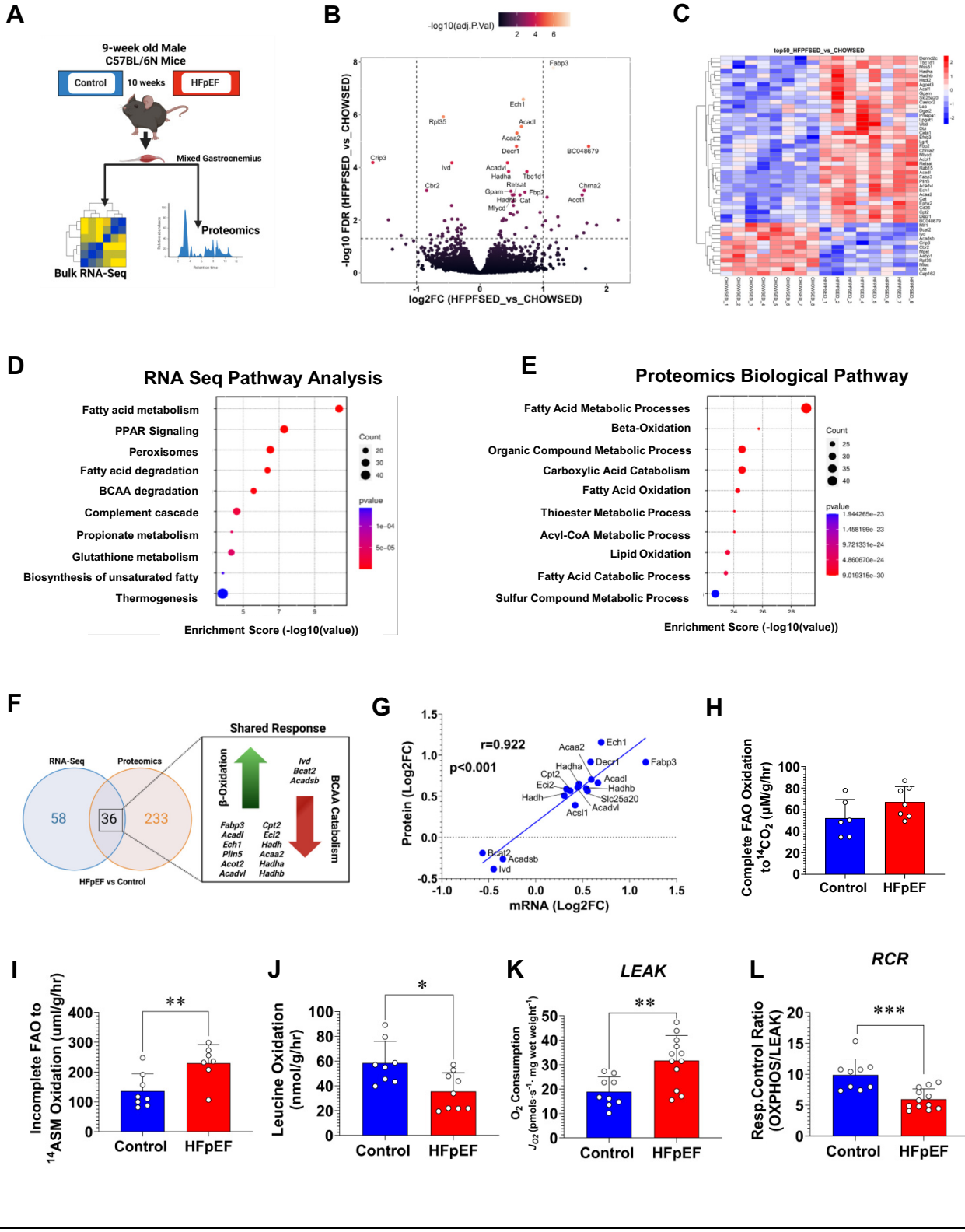


*Continued on the next page*

**FIGURE 2 Wheel Running Exercise Improves Muscle Function and Metabolic Health in HFpEF Mice**

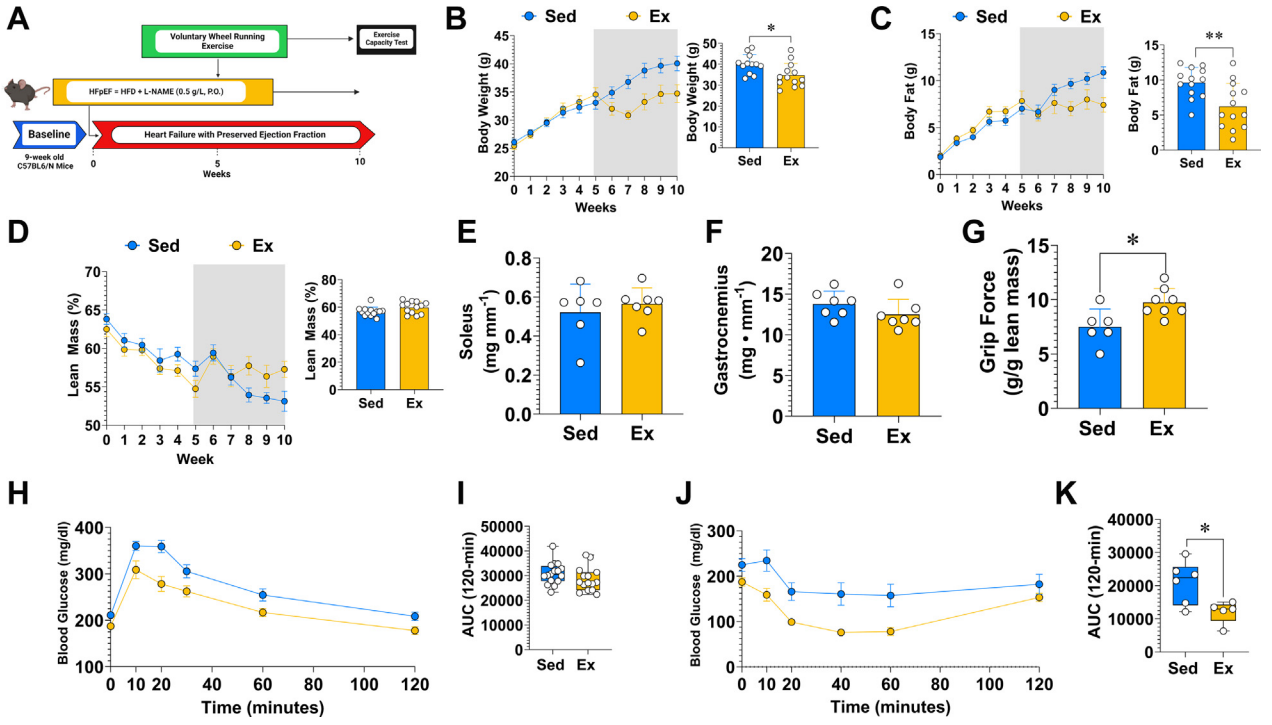


(A) Five weeks after the onset of HFpEF (HFD+L-NAME) mice were randomly assigned to the exercise (Ex) group and housed in cages with running wheels or single-housed in a standard cage to mimic a sedentary (Sed) condition. (B) Body mass, (C) body fat, and (D) lean mass were assessed weekly. The shaded area indicates the start of 5-week Ex training or Sed conditions. The adjoining bar graph represents the week 10 measurement. (E) Soleus and gastrocnemius (F) wet weight were measured immediately after sacrifice. (G) Average forelimb grip force production after 5 weeks of exercise. (H, I) Oral glucose tolerance and (J, K) insulin tolerance in Sed vs Ex mice. All data are presented as mean ± SD. An unpaired Student's *t*-test was used to determine the significance for B to J. A mixed model was used to determine the difference between glucose (G) and insulin tolerance (I). $*P < 0.05$. $**P < 0.01$. AUC = area under the curve; P.O. = orally; other abbreviations as in Figure 1.

group. Thereafter running wheels were unlocked and both groups were allowed to run ad libitum to determine exercise capacity with continuous metabolic monitoring (**Figure 3A**, Supplemental Figure 6). Analysis of whole-body energy expenditure revealed that exercise training markedly increased nonresting energy expenditure (**Figures 3B and 3C**) and wheel running energy expenditure (**Figures 3D and 3E**). During wheel running exercise, the Ex mice had a lower respiratory exchange ratio than the Sed mice

**FIGURE 1 Continued**

(A) Bulk RNA-sequencing (RNA-seq) and proteomics were performed on mixed gastrocnemius skeletal muscle after 10 weeks of chow (Control) or high-fat diet- N(ω)-nitro-L-arginine methyl ester (HFD+L-NAME) (heart failure with preserved ejection fraction [HFpEF]) (n = 8 per group). (B) Volcano plot showing the differential gene expression response between control and HFpEF mice. (C) Heatmap showing the top 50 (*P* value) differentially expressed genes between HFpEF and control. (D,E) Dot plot pathway analysis showing the significance of pathways enriched between HFpEF and control for RNA-seq and proteomics, respectively. (F) Venn diagram demonstrating the overlap between shared genes and proteins that were differentially changed between HFpEF and control skeletal muscle. (G) Linear regression demonstrating the relationship between $\log_2$ fold change (FC) in messenger RNA (mRNA) and protein. $^{14}$Carbon-oxidation (n = 6-8) of skeletal muscle (gastrocnemius) homogenates after 10 weeks of HFD+L-NAME treatment for (H) completed fatty acid oxidate (FAO) (palmitate), (I) incomplete FAO to $^{14}$acid-soluble metabolites and (J) leucine. (K) LEAK state respiration and (L) respiratory control ratio for permeabilized soleus muscle fibers (n = 9-12). All data are presented as mean ± SD. An unpaired Student's *t*-test was used to determine the significance (H toL). A false discovery rate (FDR) <0.05 with a $\log_2$ FC was used to determine significantly changed targets (I to K). Simple linear regression was used to determine significance (G). All data are presented as mean ± SD. An unpaired Student's *t*-test was used to determine significance for A to C. $*P < 0.05$, $**P < 0.01$, $***P < 0.001$. Acyl-CoA = acetyl-coenzyme A ; BCAA = branched-chain amino acid; PPAR = peroxisome proliferator-activated receptor.

**FIGURE 3** Exercise Training Increases Voluntary Exercise EE and Promotes Whole-Body Lipid Oxidation In Vivo

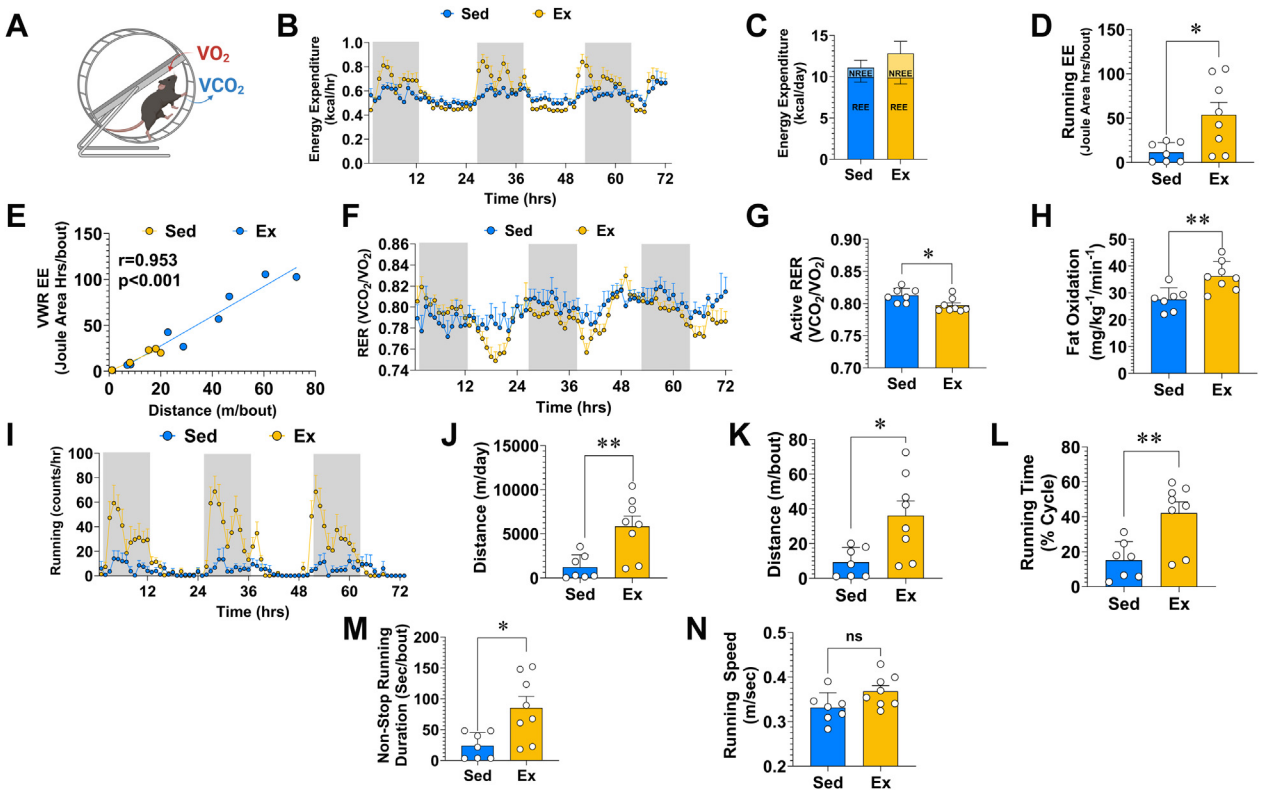


At the end of the 5-week training or sedentary period, mice were placed in metabolic cages with a locked running wheel for 3 days. After the 3-day nonexercise period, the running wheels were then unlocked to measure voluntary exercise capacity. (A) Metabolic cage analysis of oxygen uptake ($V_{O_2}$) and $CO_2$ ($V_{CO_2}$) production during periods of wheel running. (B) Three-day representation and (C) average total energy expenditure (EE). (D) EE per bout of wheel running. (E) Relationship between EE and distance per bout. (F) Three-day representation and (G) average respiratory exchange ratio (RER) during wheel running. (H) Average relative fat oxidation. (I) Three-day representation of average hourly wheel running (counts/h), (J) daily running distance, (K) running distance per bout, **(L)** the percentage of time cycle engaged in wheel running, (M) nonstop running distance per bout, (I) average running speed per bout. All data are presented as mean ± SD with 7-8 mice per group. An unpaired Student's *t*-test was used to determine significance for D, G, H, J, K, L, M, and N and simple linear regression for E. $^*P < 0.05$, $^{**}P < 0.01$.
NREE = nonresting energy expenditure; NS = not significant; REE = resting energy expenditure; VWR = voluntary wheel running; other abbreviations as in Figure 2.

did (Figures 3F and 3G), suggesting a shift toward greater fat oxidation post exercise training. Figure 3H confirms the increase in relative whole-body fat oxidation. HFpEF mice in the Ex group demonstrated superior exercise capacity in terms of running distance (Figures 3F and 3I), amount of time running (Figure 3L), and nonstopping distance (Figure 3M). Running speed was numerically increased but did not meet statistical significance ($P = 0.060$) (Figure 3N). Exercise training also increased several measurements of spontaneous physical activity (Figure 4A). Total ambulation (Figures 4B and 4C), beam breaks (Figure 4D), walking meters (Figure 4E), walking speed (Figure 4F), and proportion of time spent walking in the cage were all increased with exercise (Figure 4G). Accordingly, stillness time was reduced in exercise-trained HFpEF mice (Figure 4H).

**EXERCISE TRAINING RESCUES BCAA CATABOLIC DEFECTS.** RNA-sequencing demonstrates the up-regulation of pathways involved in peroxisome proliferator-activated receptor signaling, amino acid metabolism, and oxidative stress in skeletal muscle in HFpEF mice after exercise training (Figures 5A to 5D, Supplemental Figure 7). Exercise further increases the expression of genes associated with β-oxidation (*Acaa2, Eci1, Ppara, Acadl*) (Figure 5E, FAO portion of graph). Conversely, genes that regulate BCAA catabolism (*Bcat2, Bckdha, Ivd*) previously demonstrated to be down-regulated (Figures 1B and 1C) in HFpEF, were significantly increased with exercise training (Figure 5E). Even though immunohistochemistry did not reveal a significant ($P = 0.079$) increase in oxidative fibers of the tibialis anterior muscle after exercise training, we did detect an increase in *Myh7*

**FIGURE 4 Wheel Running Exercise Increases SPA**

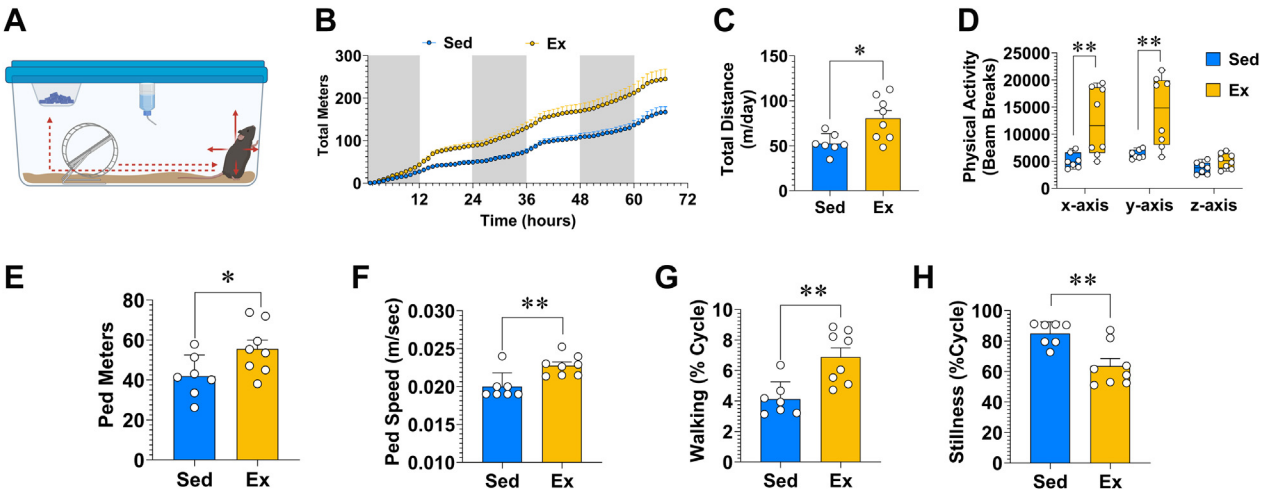


(A) Spontaneous physical activity (SPA) monitored during the "off-wheel" period. (B) Three-day representation and (C) distance in cage. (D) Physical activity is expressed as beam breaks in the x-, y-, and z-axes. Average walking (E) distance and (F) speed per cycle. (G) Percentage of time during the cycle without movement. All data are presented as mean ± SD with 7-8 mice per group. An unpaired Student's *t*-test was used to determine significance (C to H). $^{*}P < 0.05$, $^{**}P < 0.01$. Ped = pedometer; other abbreviations as in Figure 2.

gene expression of the gastrocnemius muscle (Supplemental Figure 8). Untargeted proteomics reveals biological pathways related to oxidative metabolism and the electron transport chain (ETC) (Figure 5F). Therefore, we conducted a targeted proteomic approach to determine the impact of exercise on the tricarboxylic acid cycle, ETC, and BCAA catabolic proteins. Figure 5G demonstrates the increased abundance of proteins important for fatty acid transport and β-oxidation. Proteins involved in BCAA catabolism were broadly increased (Figure 5H, Supplemental Figure 9), but the phosphorylation of branched-chained ketoacid dehydrogenase was unaltered by exercise (Supplemental Figure 10). Functionally, complete FAO (Figure 5I) increased, whereas incomplete FAO (Figure 5J) was numerically lower with exercise, but did not achieve statistical significance ($P = 0.09$). Leucine oxidation was increased between Ex and Sed HFpEF groups (Figure 5K). Pyruvate oxidation was not changed with exercise (Figure 5L). Mitochondrial respiration rates measured using carbohydrate-based substrates did not change after exercise training in gatrocnemius and soleus muscle fibers (Supplemental Figure 11).

**EXERCISE PROMOTES MITOCHONDRIAL ETC PROTEOSTASIS.** Exercise is a strong inducer of mitochondrial plasticity, biogenesis, and ETC capacity in skeletal muscle.[60] We performed a targeted analysis of the mitochondrial ETC proteome to determine the adaptability of skeletal muscle in HFpEF mice. We detected a total of 79 ETC proteins of which 18 were significantly increased by exercise (Figure 6). Consistent with other reports,[61] exercise training stimulated a broad proteomic change across all respiratory complexes with the largest increases detected in cytochrome C oxidase subunits I, II, and III (Cox1 Mtco1,2,3) (Figures 6A to 6D).

**VOLUNTARY WHEEL RUNNING EXERCISE DOES NOT ATTENUATE ELEVATED LV FILLING PRESSURE IN CARDIOMETABOLIC HFpEF.** We performed an invasive hemodynamic analysis of LV pressure and relaxation in HFpEF Sed and Ex. Exercise did not augment systolic blood pressure (Figure 7A), diastolic blood pressure (Figure 7B), tau (Figure 7C), or LVEDP (Figure 7D). Heart weight was also not different between Sed and Ex HFpEF mice (Figure 7E). However, there was a strong inverse association between kilometers of distance run per day and LVEDP (Figure 7F).

## DISCUSSION

Exercise intolerance is the defining symptom, a critical determinant of morbidity, and a risk factor for mortality in HFpEF.[22] There is mounting evidence that skeletal muscle dysfunction is a major contributor to exercise intolerance in HFpEF.[11,13-15,62] Mitochondrial dysfunction is highly associated with

**FIGURE 5** **Wheel Running Exercise Reverses Skeletal Muscle Metabolic Dysfunction in HFpEF**

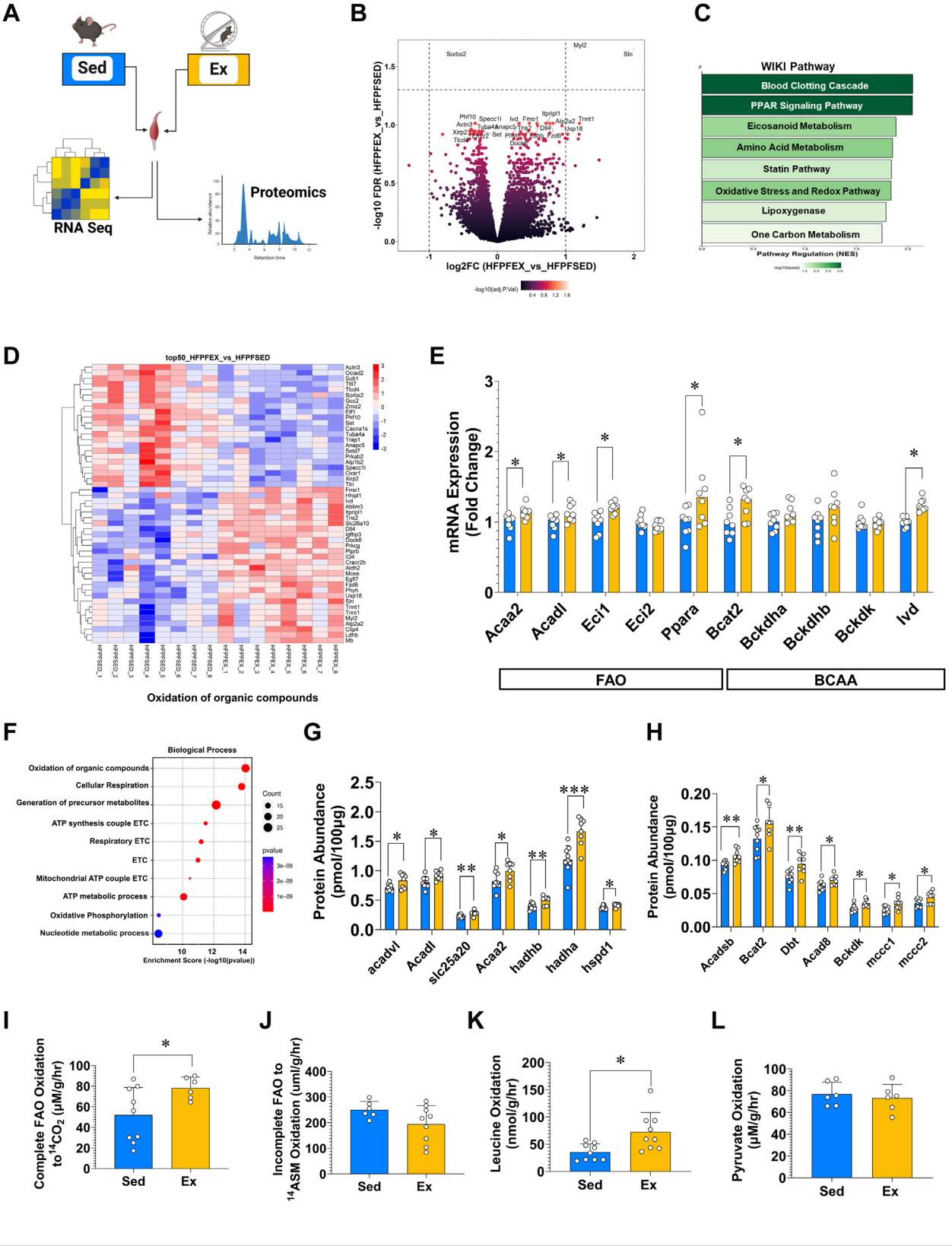


*Continued on the next page*

**FIGURE 6 Exercise Remodels the Mitochondrial ETC Proteome**

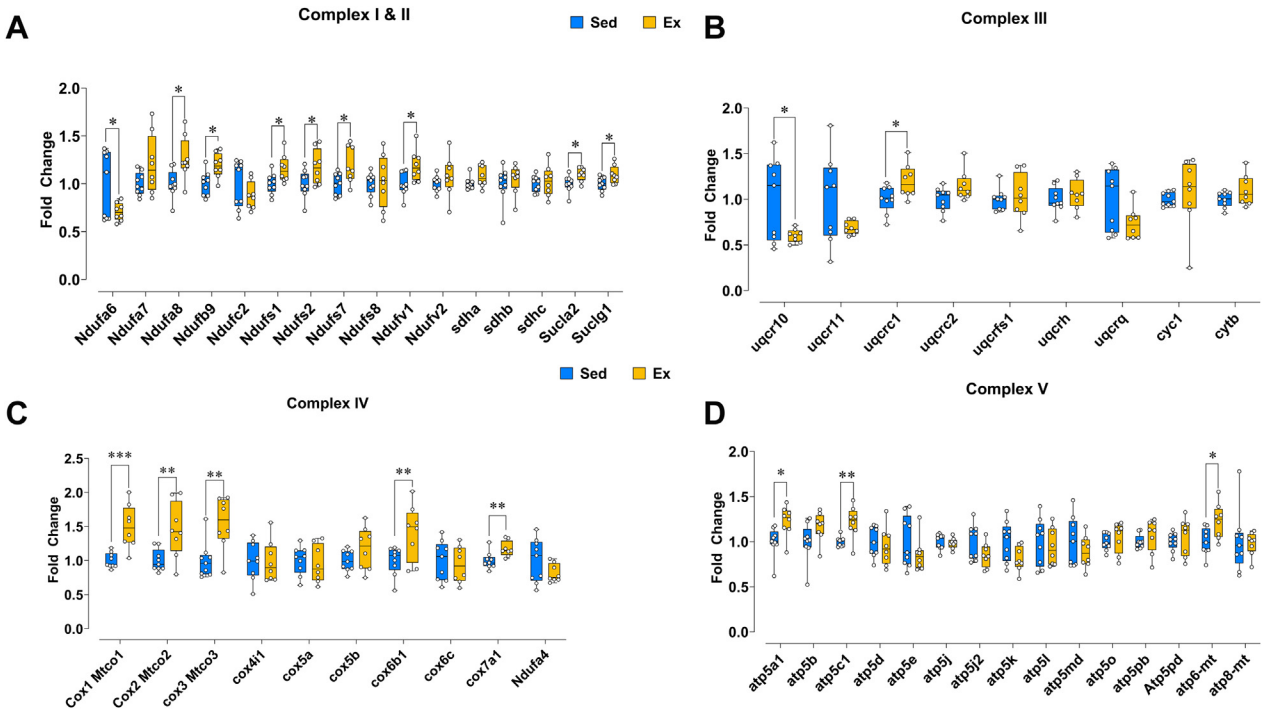


(A) Skeletal muscle (gastrocnemius) complexes I and II, (B) complex III, (C) complex IV, and (D) complex V protein abundance in HFpEF Sed and Ex mice (n = 8-9 per group). All data are presented as mean ± SD. An unpaired Student's *t*-test was used to determine the significance for A to D. *$P < 0.05$, **$P < 0.01$, ***$P < 0.001$. Abbreviations as in Figures 1, 2, and 5.

exercise intolerance in HFpEF and aging populations.[63] Our functional and multiomic approach demonstrates skeletal muscle mitochondrial dysfunction manifests primarily in excess rates of incomplete FAO in HFpEF mice (Figures 1H and 1I). Whereas this observation is consistent with the concept of mitochondrial overload in rodent models of diet-induced obesity,[41] we demonstrate this phenomenon to be exacerbated HFpEF when compared to diet-induced obesity alone (Supplemental Figures 5A and 5B). Previous reports show patients with HFpEF also have impaired cardiac fatty acid gene expression and metabolite accumulation associated with incomplete fatty acid metabolism.[14,19] The inability to completely oxidize lipids in the mitochondria is associated with the accumulation of lipid intermediates (ie, acylcarnitines).[41] These lipid species and radicals are signaling nodes for insulin resistance and oxidative stress.[41] In the obese state, a lipid represents a critical pool of substrate for exercising skeletal muscle.[64,65] We demonstrate that the inability to completely oxidize lipids in the skeletal

**FIGURE 5 Continued**

(A) Schematic overview of analysis pipeline for Sedentary and Exericse HFpEF mice. (B) Volcano plots demonstrating the change in gene expression (RNA-seq) of skeletal muscle (gastrocnemius) between Sed and Ex HFpEF mice. (C) WikiPathways (WIKI Pathway) database demonstrates regulation in response to exercise in HFpEF skeletal muscle. (D) Heatmap of top 50 differentially regulated genes (FDR $P < 0.05$) for Sed vs Ex HFpEF groups. (E) Targeted quantitative polymerase chain reaction of relevant genes from highly enriched pathways. (J) Enrichment plot of proteomic of biological pathways altered between Sed and Ex HFpEF mice. (G,H) Targeted proteomic quantification for (L) β-oxidation and BCAA catabolic peptides. $^{14}$C-oxidation (n = 6-8) of skeletal muscle (gastrocnemius) homogenates for (I) completed FAO (palmitate), (J) incomplete FAO to $^{14}$acid-soluble metabolites (ASM), (K) change in complete FAO with 10 mmol/L pyruvate, (K) leucine, and (L) pyruvate. All data are presented as mean ± SD. An FDR <0.05 with a $\log_2$ FC was used to determine a significantly alerted gene for RNA-seq (B to D). An unpaired Student's *t*-test was used to determine the significance for E, G, H, I, J, K, and L. *$P < 0.05$, **$P < 0.01$, ***$P < 0.001$. ATP = adenosine triphosphate; ETC = electron transport chain; NES = normalized enrichment score; other abbreviations as in Figures 1 and 2.

**FIGURE 7** **Wheel Running Exercise Had No Effect on Cardiac Hemodynamics**

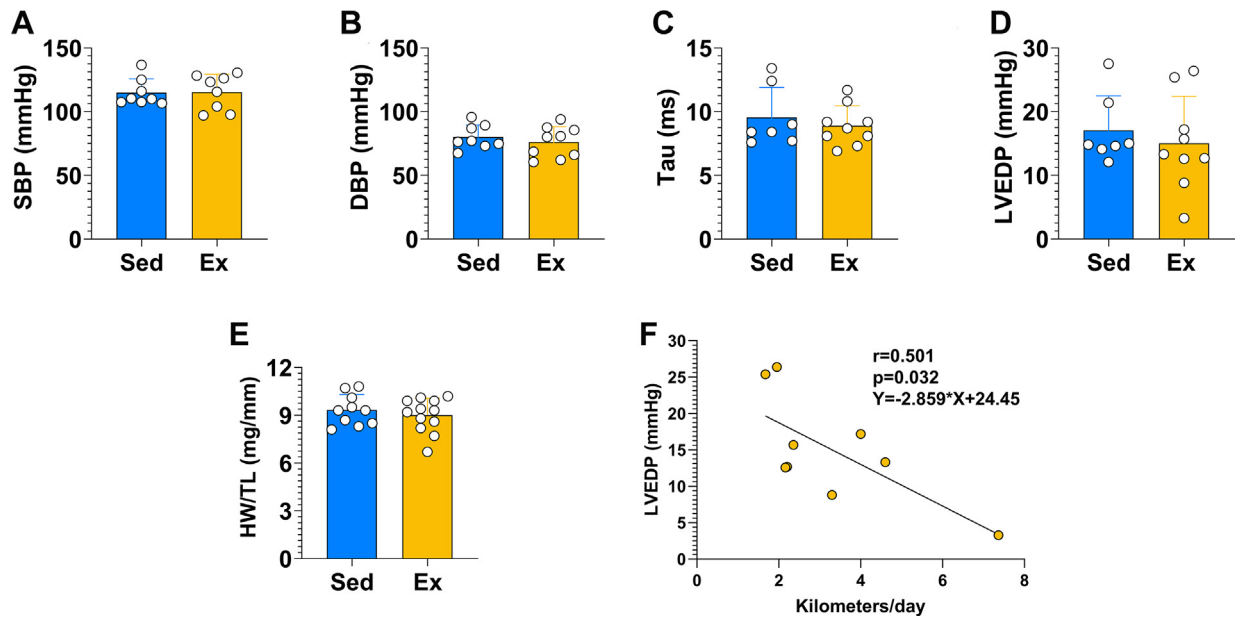


(A) Systolic blood pressure (SBP), (B) diastolic blood pressure (DBP), (C) tau, (D) left ventricular end-diastolic pressure (LVEDP), and (E) heart weight in HFpEF Sed vs Ex mice (n = 7-8 per group). (F) The relationship between daily wheel running and LVEDP. All data are presented as mean ± SD. An unpaired Student's *t*-test was used to determine the significance for A to D. (F) Simple linear regression was used to analyze LVEDP vs running distance. HW/TL = heart weight to tibial length ratio; other abbreviations as in Figure 2.

muscle is potentially an important and novel mechanism of exercise intolerance in cardiometabolic HFpEF.

BCAAs are an important substrate for skeletal muscle during rest and exercise.[66,67] During exercise, BCAAs provide NADH (via glutamate dehydrogenase) to produce adenosine triphosphate and supply tricarboxylic acid cycle intermediates through α-ketoglutarate.[67] In rodent models of obesity and insulin resistance, BCAA oxidation is shifted toward the skeletal muscle.[68] In obese patients with HFpEF, plasma BCAAs are increased, and myocardial BCAA metabolites are reduced, suggesting impaired BCAA catabolism.[20] We report a reduction in BCAA enzyme gene expression, protein abundance, and oxidation of leucine in HFpEF skeletal muscle. Consistent with previous reports, our data indicate that exercise training has a targeted effect on skeletal muscle to restore BCAA catabolism.[69-72] The phosphorylation state of the rate-limiting enzyme branched-chained ketoacid dehydrogenase was not augmented by exercise and thus cannot explain the mechanism by which BCAA oxidation is increased after exercise training. However, work by Neinast et al[68] demonstrates that in vivo BCAA flux cannot be solely determined by protein content and or phosphorylation of branched-chained ketoacid dehydrogenase. Therefore, future studies using stable isotope tracing techniques with intact model systems will be required to elucidate exercise-mediated improvements in BCAA metabolism.

Although we did not detect enhanced muscle fiber respiration, similar findings of unchanged respiration despite enhanced exercise capacity have been noted by other researchers in response to wheel running exercise.[73,74] Nonetheless, there was a broad increase of ETC proteins (**Figure 6**) after exercise training, suggesting an increase in mitochondrial protein accretion. In patients with HFpEF, reduced mitochondrial OXPHOS protein content has been reported.[75] Data from Molina et al[13] suggest that exercise intolerance is closely associated with reduced mitochondrial protein content, specifically MFN2, in HFpEF patients. Whereas our targeted analysis did not include Mfn2, we analyzed many proteins with broad coverage of the mitochondrial proteasome, advancing the previous work in this field.

Despite a dramatic improvement in exercise capacity, we did not observe any changes in cardiac hemodynamic function in response to exercise training in HFpEF mice. Interestingly, clinical investigations demonstrate significant improvements

in maximal oxygen uptake and muscle function after exercise training in HFpEF without improvements in cardiac function.[76] Work by Balmain et al[77] demonstrates that reducing hemodynamic pressure (pulmonary capillary wedge pressure) does not improve exercise capacity in HFpEF. Other groups show treatments that specifically target cardiac function (neprilysin inhibitor and angiotensin II type I inhibitor) do not alleviate skeletal muscle dysfunction or exercise intolerance in HFpEF.[78,79] These findings underscore the importance of skeletal muscle function and metabolism in the pathogenesis of exercise intolerance in HFpEF. Furthermore, the response to exercise training to improve physical capacity does not require a reduction in resting LVEDP, suggesting skeletal muscle is uncoupled from cardiac dysfunction in HFpEF.

**STUDY LIMITATIONS.** Whereas our investigation provides an in-depth analysis of skeletal muscle metabolism and the impact of exercise therapy, there are some limitations we must acknowledge. Mice in the Ex group had a lower body weight and body fat at the end of the study. Both exercise and weight loss promote numerous metabolic benefits, some of which can be attributed to negative energy balance.[80-82] At the time of sacrifice, mice in both Sed and Ex groups had not significantly fluctuated in weight during the last week, suggesting a state of relative energy balance. Future studies should carefully consider the impact of weight loss (via caloric restriction or pharmacotherapy) alone or in combination with exercise on skeletal muscle metabolism in HFpEF. Another limitation of our work is that we only used the 2-hit model of HFpEF in our study. Other cardiometabolic HFpEF models, such as the ZSF1 obese rat also demonstrate obesity, hypertension, and diastolic dysfunction. However, the ZSF1 obese rat develops obesity secondary to a leptin receptor defect-induced hyperphasia.[83] Whereas the "2-hit "mouse model of HFpEF undergoes HFD-induced obesity. The difference between lipid overload vs nutrient/caloric overload may have important implications on skeletal muscle metabolism, the development of exercise intolerance, and the impact of exercise training. Bowen et al[84] performed 8 weeks of moderate or high-intensity treadmill exercise training in ZSF1 obese rats starting at 20 weeks of age. Neither moderate nor high-intensity treadmill exercise reversed skeletal muscle capillary density or contractile dysfunction. However, future work should include a more thorough analysis of skeletal muscle metabolism and measurement of exercise capacity in response to exercise training in the ZSF1 rat model to improve the translational potential of this model.

Finally, another important consideration is our selection of exercise modality. We used voluntary wheel running because it promotes canonical aerobic exercise adaptations without stressful reinforcement measures.[85] The magnitude in which our results compare to other forms of exercise that can control for volume and intensity (forced treadmill running) or total muscle engagement (forced swimming) is an important consideration for future research. Exercise intolerance is not only characterized by skeletal muscle mitochondrial and metabolic dysfunction in HFpEF. Reduced capillarization and altered perfusion are present in patients and some animal models HFpEF.[7,12,86] Exercise involves an integrated physiological response that includes increased perfusion to the working skeletal muscle. Our investigation did not evaluate this outcome and should be considered a limitation. Other limitations of our work include the lack of aging and female sex in our mouse model. Both older age and female sex are highly represented in clinical HFpEF.[87,88] Follow-up studies should determine whether the mechanism of metabolic dysfunction we have established is altered by these important risk factors.

## CONCLUSIONS

In summary, we show that HFD and L-NAME-induced HFpEF promote mitochondrial dysfunction characterized by reduced BCAA catabolism and mishandling of fatty acid (incomplete FAO). Importantly, this 2-hit model of HFpEF shares a broad transcriptional and proteomic signature with mice exposed only to HFD. However, HFpEF mice demonstrate more severe dysregulation substrate oxidation (leucine and palmitate) and exercise intolerance. These metabolic defects, and associated exercise intolerance, are mostly reversed by exercise training. At the molecular level, the reversal of these effects appears to be predominantly related to BCAA catabolic proteins. Exercise training also partitions more lipids to undergo complete vs incomplete oxidation. Mechanistically, a further increase in gene expression and protein abundance appears to be involved in the improved metabolic capacity of skeletal muscle to oxidize lipids. Therefore, therapies targeting these metabolic mechanisms (reduced BCAA catabolism and incomplete FAO), as exercise training does, should be evaluated to treat HFpEF. Pharmacologic therapy that mimics the effects of exercise could be prescribed to patients with HFpEF to improve exercise tolerance, which could then lead to the ability of these patients to start exercising more easily, thereby synergizing between

pharmacologic and physiological approaches to improving functional status and exercise capacity.

**ACKNOWLEDGMENTS** The authors thank Dr Jarek Staszkiewicz for assistance with bioinformatic analysis. They would like to thank Dr Bernard Rees for the use of additional Oroboros O2ks, which were partly funded by the Louisiana Board of Regents (106ENH-22). The authors thank the IDeA National Resource for Quantitative Proteomics for their support of the Kinter Lab (R24GM137786).

## FUNDING SUPPORT AND AUTHOR DISCLOSURES

These studies were supported by grants from the National Institutes of Health (P20GM135002, U54GM104940, and P30AG050911 to Dr Allerton; and HL146098, HL146514, and HL151398 to Dr Lefer), William Prescott Foster Professorship (to Dr Irving), an American Heart Association Postdoctoral fellowship (20POST35200075 to Dr Li. Stampley is a recipient of the Southeastern Conference (SEC) Scholars Fund. Jake Doiron is the recipient of a training fellowship from the NIH National CCTS awarded to the University of Alabama at Birmingham as part of a TL1 Training Grant (TL1TR003106). All other authors have reported that they have no relationships relevant to the contents of this paper to disclose.

**ADDRESS FOR CORRESPONDENCE:** Dr Timothy D. Allerton, Vascular Metabolism Laboratory, Pennington Biomedical Research Center, 6400 Perkins Road, Baton Rouge, Louisiana 70808, USA. E-mail: timothy.allerton@pbrc.edu.

## PERSPECTIVES

**COMPETENCY IN MEDICAL KNOWLEDGE:** Skeletal muscle dysfunction is a major, noncardiac, factor that drives chronic exercise intolerance in cardiometabolic HFpEF. Exercise training is a frontline therapy that can improve skeletal muscle function and ameliorate exercise intolerance in HFpEF. Importantly, these improvements in exercise capacity do require significant improvements in cardiac function. Clinical investigations that have targeted cardiac function in HFpEF do not universally restore and, in some cases impair, exercise capacity in HFpEF. These studies suggest skeletal muscle dysfunction is uncoupled from cardiac dysfunction in HFpEF and is possibly an independent target for therapy.

**TRANSLATIONAL OUTLOOK:** We demonstrate mitochondrial dysfunction, and impaired lipid and BCAA metabolism are metabolic signatures of skeletal muscle in a 2-hit mouse model of cardiometabolic HFpEF. Exercise training in the form of voluntary wheel running reversed many of these metabolic deficiencies and improved exercise capacity in this model. Exercise training in patients with HFpEF also improves exercise intolerance independent of improvements in cardiac function. Future studies are needed to determine whether similar metabolic adaptations in skeletal muscle after exercise are necessary to improve exercise tolerance in patients with HFpEF.

## REFERENCES

**1.** Borlaug BA, Sharma K, Shah SJ, Ho JE. Heart failure with preserved ejection fraction: JACC Scientific Statement. *J Am Coll Cardiol*. 2023;81(18):1810–1834.

**2.** Virani SS, Alonso A, Benjamin EJ, et al. Heart disease and stroke statistics—2020 update a report from the American Heart Association. *Circulation*. 2020;141(9):e139–e596.

**3.** Tsao CW, Lyass A, Enserro D, et al. Temporal trends in the incidence of and mortality associated with heart failure with preserved and reduced ejection fraction. *JACC Heart Fail*. 2018;6(8):678–685.

**4.** Shah KS, Xu H, Matsouaka RA, et al. Heart failure with preserved, borderline, and reduced ejection fraction: 5-year outcomes. *J Am Coll Cardiol*. 2017;70(20):2476–2486.

**5.** Gerber Y, Weston SA, Redfield MM, et al. A contemporary appraisal of the heart failure epidemic in Olmsted County, Minnesota, 2000 to 2010. *JAMA Intern Med*. 2015;175(6):996–1004.

**6.** Obokata M, Reddy YNV, Pislaru SV, Melenovsky V, Borlaug BA. Evidence supporting the existence of a distinct obese phenotype of heart failure with preserved ejection fraction. *Circulation*. 2017;136(1):6–19.

**7.** Zamani P, Proto EA, Mazurek JA, et al. Peripheral determinants of oxygen utilization in heart failure with preserved ejection fraction: central role of adiposity. *JACC Basic Transl Sci*. 2020;5(3):211–225.

**8.** Packer M, Lam CSP, Lund LH, Maurer MS, Borlaug BA. Characterization of the inflammatory-metabolic phenotype of heart failure with a preserved ejection fraction: a hypothesis to explain influence of sex on the evolution and potential treatment of the disease. *Eur J Heart Fail*. 2020;22(9):1551–1567.

**9.** Kitzman DW, Lam CSP. Obese heart failure with preserved ejection fraction phenotype: from pariah to central player. *Circulation*. 2017;136(1):20–23.

**10.** Haykowsky MJ, Brubaker PH, John JM, Stewart KP, Morgan TM, Kitzman DW. Determinants of exercise intolerance in elderly heart failure patients with preserved ejection fraction. *J Am Coll Cardiol*. 2011;58(3):265–274.

**11.** Nayor M, Houstis NE, Namasivayam M, et al. Impaired exercise tolerance in heart failure with preserved ejection fraction: quantification of multiorgan system reserve capacity. *JACC Heart Fail*. 2020;8(8):605–617.

**12.** Haykowsky MJ, Kouba EJ, Brubaker PH, Nicklas BJ, Eggebeen J, Kitzman DW. Skeletal muscle composition and its relation to exercise intolerance in older patients with heart failure and preserved ejection fraction. *Am J Cardiol*. 2014;113(7):1211–1216.

**13.** Molina AJA, Bharadwaj MS, Van Horn C, et al. Skeletal muscle mitochondrial content, oxidative capacity, and Mfn2 expression are reduced in older patients with heart failure and preserved ejection fraction and are related to exercise intolerance. *JACC Heart Fail*. 2016;4(8):636–645.

**14.** Bekfani T, Bekhite Elsaied M, Derlien S, et al. Skeletal muscle function, structure, and metabolism in patients with heart failure with reduced ejection fraction and heart failure with preserved ejection fraction. *Circ Heart Fail*. 2020;13(12):E007198.

**15.** Scandalis L, Kitzman DW, Nicklas BJ, et al. Skeletal muscle mitochondrial respiration and exercise intolerance in patients with heart failure with preserved ejection fraction. *JAMA Cardiol*. 2023;8(6):575.

**16.** Weiss K, Schär M, Panjrath GS, et al. Fatigability, exercise intolerance, and abnormal skeletal muscle energetics in heart failure. *Circ Heart Fail*. 2017;10(7):e004129.

**17.** Zordoky BN, Sung MM, Ezekowitz J, et al. Metabolomic fingerprint of heart failure with preserved ejection fraction. *PLoS One*. 2015;10(5):e0124844. https://doi.org/10.1371/journal.pone.0124844

**18.** Bekfani T, Bekhite M, Neugebauer S, et al. Metabolomic profiling in patients with heart failure and exercise intolerance: kynurenine as a potential biomarker. *Cells*. 2022;11(10):1674.

**19.** Hunter WG, Kelly JP, Mcgarrah RW, et al. Metabolomic profiling identifies novel circulating biomarkers of mitochondrial dysfunction differentially elevated in heart failure with preserved versus reduced ejection fraction: evidence for shared metabolic impairments in clinical heart failure. *J Am Heart Assoc*. 2016;5(8):e003190.

**20.** Hahn VS, Petucci C, Kim M-S, et al. Myocardial metabolomics of human heart failure with preserved ejection fraction. *Circulation*. 2023;147(15):1147–1161.

**21.** Ramirez MF, Lau ES, Parekh JK, et al. Obesity-related biomarkers are associated with exercise intolerance and HFpEF. *Circ Heart Fail*. 2023;16(11):e010618.

**22.** Nadruz W, West E, Sengeløv M, et al. Prognostic value of cardiopulmonary exercise testing in heart failure with reduced, midrange, and preserved ejection fraction. *J Am Heart Assoc*. 2017;6(11):e0060000.

**23.** Guazzi M, Myers J, Arena R. Cardiopulmonary exercise testing in the clinical and prognostic assessment of diastolic heart failure. *J Am Coll Cardiol*. 2005;46(10):1883–1890.

**24.** Sachdev V, Sharma K, Keteyian SJ, et al. Supervised exercise training for chronic heart failure with preserved ejection fraction: a scientific statement from the American Heart Association and American College of Cardiology. *Circulation*. 2023;147(16):e699–e715.

**25.** Orimoloye OA, Kambhampati S, Hicks AJ, et al. Higher cardiorespiratory fitness predicts long-term survival in patients with heart failure and preserved ejection fraction: the Henry Ford exercise Testing (FIT) project. *Arch Med Sci*. 2019;15(2):350–358.

**26.** Kosiborod MN, Abildstrøm SZ, Borlaug BA, et al. Semaglutide in patients with heart failure with preserved ejection fraction and obesity. *N Engl J Med*. 2023;389(12):1069–1084.

**27.** Solomon SD, McMurray JJV, Claggett B, et al. Dapagliflozin in heart failure with mildly reduced or preserved ejection fraction. *N Engl J Med*. 2022;387(12):1089–1098.

**28.** Nassif ME, Windsor SL, Borlaug BA, et al. The SGLT2 inhibitor dapagliflozin in heart failure with preserved ejection fraction: a multicenter randomized trial. *Nat Med*. 2021;27(11):1954–1960.

**29.** Anker SD, Butler J, Filippatos G, et al. Empagliflozin in heart failure with a preserved ejection fraction. *N Engl J Med*. 2021;385(16):1451–1461.

**30.** Kitzman DW, Brubaker PH, Morgan TM, Stewart KP, Little WC. Exercise training in older patients with heart failure and preserved ejection fraction: a randomized, controlled, single-blind trial. *Circ Heart Fail*. 2010;3(6):659–667.

**31.** Edelmann F, Gelbrich G, Dngen HD, et al. Exercise training improves exercise capacity and diastolic function in patients with heart failure with preserved ejection fraction: results of the Ex-DHF (exercise training in diastolic heart failure) pilot study. *J Am Coll Cardiol*. 2011;58(17):1780–1791.

**32.** Kitzman DW, Brubaker PH, Herrington DM, et al. Effect of endurance exercise training on endothelial function and arterial stiffness in older patients with heart failure and preserved ejection fraction: a randomized, controlled, single-blind trial. *J Am Coll Cardiol*. 2013;62(7):584–592.

**33.** Tong D, Schiattarella GG, Jiang N, et al. Female sex is protective in a preclinical model of heart failure with preserved ejection fraction. *Circulation*. 2019;140(21):1769–1771.

**34.** Tong D, Schiattarella GG, Jiang N, et al. NAD+ repletion reverses heart failure with preserved ejection fraction. *Circ Res*. 2021;128(11):1629–1641.

**35.** Schiattarella G, Altamirano F, Tong D, et al. Nitrosative stress drives heart failure with preserved ejection fraction. *Nature*. 2019;568(7752):351–356.

**36.** Schiattarella GG, Altamirano F, Kim SY, et al. Xbp1s-FoxO1 axis governs lipid accumulation and contractile performance in heart failure with preserved ejection fraction. *Nat Commun*. 2021;12(1):1684.

**37.** LaPenna KB, Li Z, Doiron JE, et al. Combination sodium nitrite and hydralazine therapy attenuates heart failure with preserved ejection fraction severity in a "2-hit" murine model. *J Am Heart Assoc*. 2023;12(4):e028480.

**38.** Jaquie E, Acheson K, Schutz Y. Assessment of energy expenditure and fuel utilization in man. *Annu Rev Nutra*. 1987;7:187–208.

**39.** Allerton TD, Kowalski G, Stampley J, et al. An ethanolic extract of artemisia dracunculus l. enhances the metabolic benefits of exercise in diet-induced obese mice. *Med Sci Sport Exec*. 2021;53(4):712–723.

**40.** Lark DS, Kwan JR, McClatchey PM, et al. Reduced nonexercised activity attenuates negative energy balance in mice engaged in voluntary exercise. *Diabetes*. 2018;67(5):831–840.

**41.** Koves TR, Ussher JR, Noland RC, et al. Mitochondrial overload and incomplete fatty acid oxidation contribute to skeletal muscle insulin resistance. *Cell Meta*. 2008;7(1):45–56.

**42.** Muoio DM, Noland RC, Kovalik J-P, et al. Muscle-specific deletion of carnitine acetyltransferase compromises glucose tolerance and metabolic flexibility. *Cell Meta*. 2012;15(5):764–777.

**43.** Noland RC, Koves TR, Seiler SE, et al. Carnitine insufficiency caused by aging and overnutrition compromises mitochondrial performance and metabolic control. *J Biol Chem*. 2009;284(34):22840–22852.

**44.** Noland RC, Thyfault JP, Henes ST, et al. Artificial selection for high-capacity endurance running is protective against high-fat diet-induced insulin resistance. *Am J Physiol Endocrinol Metab*. 2007;293(1):e31–e41.

**45.** Fuller SE, Huang TY, Simon J, et al. Low-intensity exercise induces acute shifts in liver and skeletal muscle substrate metabolism but not chronic adaptations in tissue oxidative capacity. *J Appl Physiol*. 2019;127(1):143–156.

**46.** Wicks SE, Vandanmagsar B, Haynie KR, et al. Impaired mitochondrial fat oxidation induces adaptive remodeling of muscle metabolism. *Proc Natl Acad Sci U S A*. 2015;112(25):e3300–e3309.

**47.** Doerrier C, Garcia-Souza LF, Krumschnabel G, Wohlfarter Y, Mészáros AT, Gnaiger E. High-resolution fluorespirometry and OXPHOS protocols for human cells, permeabilized fibers from small biopsies of muscle, and isolated mitochondria. *Methods Mol Biol*. 2018;1782:31–70.

**48.** Hahn D, Kumar RA, Ryan TE, Ferreira LF. Mitochondrial respiration and H2O2 emission in saponin-permeabilized murine diaphragm fibers: optimization of fiber separation and comparison to limb muscle. *Am J Physiol Cell Physiol*. 2019;317(4):C665–C673.

**49.** Brunetta HS, Petrick HL, Vachon B, Nunes EA, Holloway GP. Insulin rapidly increases skeletal muscle mitochondrial ADP sensitivity in the absence of a high lipid environment. *Biochem J*. 2021;478(13):2539–2553.

**50.** Allerton TD, Kowalski G, Hang H, Stephens J. Dynamic glucose disposal is driven by reduced endogenous glucose production in response to voluntary wheel running: a stable isotope approach. *Am J Physiol Metab*. 2020;319(1):E2–E10.

**51.** Huang T-Y, Linden MA, Fuller SE, et al. Combined effects of a ketogenic diet and exercise training alter mitochondrial and peroxisomal substrate oxidative capacity in skeletal muscle. *Am J Physiol Metab*. 2021;320(6):E1053–E1067.

**52.** Ghosh S, Wicks SE, Vandanmagsar B, et al. Extensive metabolic remodeling after limiting mitochondrial lipid burden is consistent with an improved metabolic health profile. *J Biol Chem*. 2019;294(33):12313–12327.

**53.** Warfel JD, Elks CM, Bayless DS, et al. Rats lacking Ucp1 present a novel translational tool for the investigation of thermogenic adaptation during cold challenge. *Acta Physiol*. 2023;238(1):e13935. https://doi.org/10.1111/apha.13935

**54.** Linden MA, Burke SJ, Pirzadah HA, et al. Pharmacological inhibition of lipolysis prevents adverse metabolic outcomes during glucocorticoid administration. *Mol Metab*. 2023;74:101751. https://doi.org/10.1016/j.molmet.2023.101751

**55.** Gouspillou G, Sgarioto N, Norris B, et al. The relationship between muscle fiber type-specific PGC-1α content and mitochondrial content varies between rodent models and humans. *PLoS One*. 2014;9(8):e103044.

**56.** Leuchtmann AB, Afifi Y, Ritz D, Handschin C. Effects of high-resistance wheel running on hallmarks of endurance and resistance training adaptations in mice. *Physiol Rep*. 2023;11(11):e15701.

**57.** Fernández-Verdejo R, Ravussin E, Speakman JR, Galgani JE. Progress and challenges in analyzing rodent energy expenditure. *Nat Methods*. 2019;16(9):797–799.

**58.** Tschöp MH, Speakman JR, Arch JRS, et al. A guide to analysis of mouse energy metabolism. *Nat Methods*. 2011;9(1):57–63.

**59.** Smolgovsky S, Bayer AL, Kaur K, et al. Impaired T cell IRE1α/XBP1 signaling directs inflammation in experimental heart failure with

preserved ejection fraction. *J Clin Invest*. 2023;133(24):e171874.

**60.** Holloszy JO, Coyle EF. Adaptations of skeletal muscle to endurance exercise and their metabolic consequences. *J Appl Physiol*. 2016;121(4):831–837.

**61.** Gonzalez-Franquesa A, Stocks B, Chubanava S, et al. Mass-spectrometry-based proteomics reveals mitochondrial supercomplexome plasticity. *Cell Rep*. 2021;35(8):109180. https://doi.org/10.1016/j.celrep.2021.109180

**62.** Kitzman DW, Nicklas B, Kraus WE, et al. Skeletal muscle abnormalities and exercise intolerance in older patients with heart failure and preserved ejection fraction. *Am J Physiol Heart Circ Physiol*. 2014;306(9):H1364–H1370.

**63.** Coen PM, Jubrias SA, Distefano G, et al. Skeletal muscle mitochondrial energetics are associated with maximal aerobic capacity and walking speed in older adults. *J Gerontol A Biol Sci Med Sci*. 2013;68(4):447–455.

**64.** Goodpaster BH, Theriault R, Watkins SC, Kelley DE. Intramuscular lipid content is increased in obesity and decreased by weight loss. *Metabolism*. 2000;49(4):467–472.

**65.** Goodpaster BH, He J, Watkins S, Kelley DE. Skeletal muscle lipid content and insulin resistance: evidence for a paradox in endurance-trained athletes. *J Clin Endocrinol Metab*. 2001;86(12):5755–5761.

**66.** Hagg SA, Morse EL, Adibi SA. Effect of exercise on rates of oxidation, turnover, and plasma clearance of leucine in human subjects. *Am J Physiol*. 1982;242(6):E407–E410.

**67.** She P, Zhou Y, Zhang Z, Griffin K, Gowda K, Lynch CJ. Disruption of BCAA metabolism in mice impairs exercise metabolism and endurance. *J Appl Physiol*. 2010;108(4):941–949.

**68.** Neinast MD, Jang C, Hui S, et al. Quantitative analysis of the whole-body metabolic fate of branched-chain amino acids. *Cell Metab*. 2019;29(2):417–429.e4.

**69.** Petrick HL, Holloway GP. The regulation of mitochondrial substrate utilization during acute exercise. *Curr Opin Physiol*. 2019;10:75–80.

**70.** Smith JAB, Murach KA, Dyar KA, Zierath JR. Exercise metabolism and adaptation in skeletal muscle. *Nat Rev Mol Cell Biol*. 2023;24(9):607–632.

**71.** McGee SL, Hargreaves M. Exercise adaptations: molecular mechanisms and potential targets for therapeutic benefit. *Nat Rev Endocrinol*. 2020;16(9):495–505.

**72.** Howarth KR, Burgomaster KA, Phillips SM, Gibala MJ. Exercise training increases branched-chain oxoacid dehydrogenase kinase content in human skeletal muscle. *Am J Physiol Regul Integr Comp Physiol*. 2007;293(3):R1335–R1341.

**73.** Grassi B, Majerczak J, Bardi E, et al. Exercise training in Tgαq*44 mice during the progression of chronic heart failure: cardiac vs. peripheral (soleus muscle) impairments to oxidative metabolism. *J Appl Physiol*. 2017;123(2):326–336.

**74.** McGowan EM, Ehrlicher SE, Stierwalt HD, Robinson MM, Newsom SA. Impact of 4 weeks of Western diet and aerobic exercise training on whole-body phenotype and skeletal muscle mitochondrial respiration in male and female mice. *Physiol Rep*. 2022;10(24):e15543.

**75.** Sanders-Van Wijk S, Tromp J, Beussink-Nelson L, et al. Proteomic evaluation of the comorbidity-inflammation paradigm in heart failure with preserved ejection fraction results from the PROMIS-HFpEF study. *Circulation*. 2020;142(21):2029–2044.

**76.** Haykowsky MJ, Brubaker PH, Stewart KP, Morgan TM, Eggebeen J, Kitzman DW. Effect of endurance training on the determinants of peak exercise oxygen consumption in elderly patients with stable compensated heart failure and preserved ejection fraction. *J Am Coll Cardiol*. 2012;60(2):120–128.

**77.** Balmain BN, Tomlinson AR, MacNamara JP, et al. Reducing pulmonary capillary wedge pressure during exercise exacerbates exertional dyspnea in patients with heart failure with preserved ejection fraction: implications for V/Q̇ mismatch. *Chest*. 2023;164(3):686–699.

**78.** Espino-Gonzalez E, Tickle PG, Altara R, et al. Caloric restriction rejuvenates skeletal muscle growth in heart failure with preserved ejection fraction. *JACC Basic Transl Sci*. 2024;9(2):223–240.

**79.** Solomon SD, McMurray JJV, Anand IS, et al. Angiotensin-neprilysin inhibition in heart failure with preserved ejection fraction. *N Engl J Med*. 2019;381(17):1609–1620.

**80.** Black SE, Mitchell E, Freedson PS, Chipkin SR, Braun B. Improved insulin action following short-term exercise training: role of energy and carbohydrate balance. *J Appl Physiol*. 2005;99(6):2285–2293.

**81.** Fisher G, Gower BA, Ovalle F, Behrens CE, Hunter GR. Acute effects of exercise intensity on insulin sensitivity under energy balance. *Med Sci Sports Exerc*. 2019;51(5):988–994.

**82.** Menshikova EV, Ritov VB, Toledo FGS, Ferrell RE, Goodpaster BH, Kelley DE. Effects of weight loss and physical activity on skeletal muscle mitochondrial function in obesity. *Am J Physiol Endocrinol Metab*. 2005;288(4):E818–E825.

**83.** Nguyen ITN, Brandt MM, van de Wouw J, et al. Both male and female obese ZSF1 rats develop cardiac dysfunction in obesity-induced heart failure with preserved ejection fraction. *PLoS One*. 2020;15(5):e0232399.

**84.** Bowen TS, Herz C, Rolim NPL, et al. Effects of endurance training on detrimental structural, cellular, and functional alterations in skeletal muscles of heart failure with preserved ejection fraction. *J Card Fail*. 2018;24(9):603–613.

**85.** Poole DC, Copp SW, Colburn TD, et al. Guidelines for animal exercise and training protocols for cardiovascular studies. *Am J Physiol Heart Circ Physiol*. 2020;318(5):H1100–H1138.

**86.** Espino-Gonzalez E, Tickle PG, Benson AP, et al. Abnormal skeletal muscle blood flow, contractile mechanics and fibre morphology in a rat model of obese-HFpEF. *J Physiol*. 2021;599(3):981–1001.

**87.** Sotomi Y, Hikoso S, Nakatani D, et al. Sex differences in heart failure with preserved ejection fraction. *J Am Heart Assoc*. 2021;10(5):e018574.

**88.** Lau ES, Cunningham T, Hardin KM, et al. Sex differences in cardiometabolic traits and determinants of exercise capacity in heart failure with preserved ejection fraction. *JAMA Cardiol*. 2020;5(1):30–37.

**KEY WORDS** branched-chained amino acids, exercise, heart failure with preserved ejection fraction, metabolism, mitochondria

**APPENDIX** For supplemental figures, please see the online version of this paper.